The actin-binding protein UNC-115 is an effector of Rac signaling during axon pathfinding in *C. elegans*

Eric C. Struckhoff and Erik A. Lundquist*

Department of Molecular Biosciences, University of Kansas, 1200 Sunnyside Avenue, Lawrence, KS 66045-7534, USA
*Author for correspondence (e-mail: erikl@ku.edu)

SUMMARY

Rac GTPases control cell shape by regulating downstream effectors that influence the actin cytoskeleton. UNC-115, a putative actin-binding protein similar to human abLIM/limatin, has previously been implicated in axon pathfinding. We have discovered the role of UNC-115 as a downstream cytoskeletal effector of Rac signaling in axon pathfinding. We show that *unc-115* double mutants with *ced-10 Rac*, *mig-2 Rac* or *unc-73 GEF* but not with *rac-2/3 Rac* displayed synthetic axon pathfinding defects, and

that loss of *unc-115* function suppressed the formation of ectopic plasma membrane extensions induced by constitutively-active *rac-2* in neurons. Furthermore, we show that UNC-115 can bind to actin filaments. Thus, UNC-115 is an actin-binding protein that acts downstream of Rac signaling in axon pathfinding.

Key words: Rac, UNC-115, Actin-binding protein, Axon pathfinding

INTRODUCTION

Rac GTPases, members of the Rho-family of small GTPases that also includes Rho and Cdc42, are central regulators of cellular morphogenesis, including axon pathfinding (reviewed by Dickson, 2001; Hall, 1998; Luo, 2000; Zigmond, 1996). Three *C. elegans* Racs, CED-10, MIG-2 and RAC-2/3, have overlapping roles in axon pathfinding and cell migration (Lundquist et al., 2001; Wu et al., 2002) and *ced-10* and *mig-2* are required redundantly for vulval epithelial morphogenesis (Kishore and Sundaram, 2002) and P-cell migration (Wu et al., 2002). Rac redundancy is conserved in *Drosophila*, where three Racs (Rac1, Rac2 and Mtl) have overlapping functions in axon pathfinding, myoblast fusion and epithelial morphogenesis (Hakeda-Suzuki et al., 2002; Ng et al., 2002). Although Rac function is redundant in some processes, *C. elegans* Racs have individual requirements in other processes. CED-10 is required for phagocytosis of cells undergoing programmed cell death and for the migration of the distal tip cells of the hermaphrodite gonad (Reddien and Horvitz, 2000), and MIG-2 is required for the migration of the Q neuroblast descendants and the distal tip cells (Zipkin et al., 1997). Redundancy of Rac function is likely to be conserved in vertebrates, which also have multiple Rac genes (Didsbury et al., 1989; Haataja et al., 1997). However, mouse *Rac1* is required individually for gastrulation and cell migration during development (Sugihara et al., 1998) and mouse *Rac2* is required for neutrophil migration (Roberts et al., 1999). Thus, metazoan genomes contain multiple Rac genes that have distinct as well as overlapping roles in a variety of morphogenetic events in vivo. Despite redundancy of Rac function in axon development, gain-of-function constitutively

active and dominant-negative Racs perturb axon pathfinding and cell migration in *C. elegans*, *Drosophila* and mouse (Lundquist et al., 2001; Luo et al., 1996; Luo et al., 1994; Zipkin et al., 1997).

Like other Ras superfamily GTPases, Racs cycle between a GTP-bound active state and a GDP-bound inactive state (Bourne et al., 1991). Molecules that regulate Rho GTPase activity include GTP exchange factors (GEFs), which stimulate exchange of GDP for GTP, promoting the active state (Kaibuchi et al., 1999). A number of dbl-homology (DH) GEFs have been implicated in controlling Rac activity, including UNC-73 Trio (Bellanger et al., 1998; Steven et al., 1998), which acts with each of the three Racs in *C. elegans* and *Drosophila* axon pathfinding in vivo (Awasaki et al., 2000; Bateman et al., 2000; Liebl et al., 2000; Lundquist et al., 2001; Newsome et al., 2000).

In the developing nervous system, growth cones, which are dynamic sensorimotor structures at the distal tip of extending axons, sense and respond to extracellular guidance cues by modulating their actin cytoskeletons, resulting in changes in direction of outgrowth (Tessier-Lavigne and Goodman, 1996). Growth cones are composed of lamellipodia and filopodia, which are dynamic, actin-based plasma membrane extensions that underlie outgrowth and guidance (Letourneau, 1996). Rac GTPases control cell shape at least in part by regulating the structure and dynamics of the actin cytoskeleton (Hall, 1998) and Rac activity can induce lamellipodia in cultured cells (Ridley et al., 1992). Recent studies have identified a number of downstream Rac effector molecules that adapt Rac activity to the actin cytoskeleton (Bishop and Hall, 2000), some of which involve activation of the actin-nucleating Arp2/3 complex. For example, Rac interacts with the adapter protein

IRSp53 which in turn links the Arp2/3 potentiator WAVE2 (Takenawa and Miki, 2001), and Rac1 along with the adapter protein Nck acitvate the Arp2/3 potentiator Scar/WAVE (Eden et al., 2002). Furthermore, the actin-interacting protein cortactin, also an Arp2/3 activator (Weaver et al., 2001), has been implicated as downstream Rac effector (Weed et al., 1998). Distinct mechanisms involve Rac interaction with p21-activated kinase, which in turn can influence the cytoskeletal effector merlin (Kissil et al., 2002; Xiao et al., 2002), and potential Rac regulation of the actin-binding protein gelsolin (Azuma et al., 1998). Thus, Rac activity can influence the actin cytoskeleton by a variety of pathways, possibly reflecting the multiple and overlapping functions of Racs in development. Undoubtedly, many downstream cytoskeletal effectors of Racs remain to be identified. Rac activity in different morphogenetic events might be controlled by different combinations of upstream Rac regulators (GEFs) and downstream cytoskeletal effectors. Mechanisms by which multiple Rac regulators, Racs and downstream effectors control different morphogenetic events in vivo remain unclear.

In this work we provide evidence that UNC-115 is a downstream Rac effector in *C. elegans* axon pathfinding. UNC-115 is similar to the human actin-binding protein abLIM/limatin (Roof et al., 1997) and is involved in axon pathfinding (Lundquist et al., 1998). We show that UNC-115 acts with the Racs and UNC-73/Trio GEF in axon pathfinding: UNC-115 acts in parallel to CED-10 and MIG-2, possibly in the RAC-2/3 pathway, and UNC-115 is required for the effects of constitutively active RAC-2 on axon morphogenesis. Furthermore, we show that UNC-115 is an actin-binding protein, suggesting that UNC-115 is a new downstream cytoskeletal effector of Rac signaling that acts specifically in the RAC-2 branch of the triply-redundant Rac pathway in axon pathfinding.

MATERIALS AND METHODS

General genetic methods

Nematodes were cultured by standard techniques (Brenner, 1974; Sulston and Hodgkin, 1988). All experiments were performed at 20°C. The following mutations were used.

LGI: *unc-73(e936, rh40)*, *kyIs5[ceh-23::gfp, lin-15(+)]*

LGIV: *ced-10(n1993)*, *dpy-13(e184)*, *lqIs3[osm-6::gfp, lin-15(+)]*

LGX: *unc-115(mn481, ky275)*, *mig-2(mu28, rh17, gm38 mu133)*, *lin-15(n765)*, *lqIs2[osm-6::gfp, lin-15(+)]*, *lqIs10[ceh-10::gfp, lin-15(+)]*, *kyIs4[ceh-23::gfp, lin-15(+)]*

Germline transformation of nematodes was performed by standard techniques (Mello and Fire, 1995) using *lin-15(n765)* mutants and *lin-15(+)* DNA (Clark et al., 1994) as a marker for co-transformation. Extrachromosomal arrays were integrated into the genome using trimethylpsoralen/UV mutagenesis (Anderson, 1995) and standard techniques (Mello and Fire, 1995). RNAi was performed by dsRNA injection (1 μg/μl) into the body cavity or gonad as described (Fire et al., 1998).

Analysis of CAN and PDE axon pathfinding and CAN cell migration

CAN axon morphology and cell position was scored using the integrated *ceh-23::gfp* transgenes *kyIs4 X* and *kyIs5 I*, or the integrated *ceh-10::gfp* transgene *lqIs10 X*, as described (Lundquist et al., 2001). A posterior CAN axon was scored as mutant if, because of premature termination or misguidance, the axon failed to extend further than half the distance between the vulva and the phasmid neurons in the tail (approximately to the region of the postdeirid ganglion). CAN cell migration was scored as mutant if the CAN cell body was greater than two CAN cell body-widths from the vulva.

PDE morphology was examined in animals harboring the integrated *osm-6::gfp* transgenes *lqIs3 IV* and *lqIs2 X* that were expressed in all ciliated sensory neurons, including PDE. A PDE axon was scored as having a pathfinding defect if, because of premature termination or axon wandering, the axon failed to reach the VNC. A PDE axon was scored as exhibiting ectopic axons if one or more ectopic axons were seen emanating from the normal axon or from the PDE cell body. A PDE cell was scored as having abnormal cellular morphology if sheet-like membrane extensions and/or finger-like membrane extensions were observed anywhere on the cell, including on the axons, dendrites and cell bodies. Each genotype was scored on at least three separate occasions, and >100 animals were scored. Twice the standard error of the proportion (percentage) is displayed in the tables. Genetic interactions were considered synthetic (the genes have redundant, overlapping functions) when the proportion of defects in the double mutant was greater than the additive effects of each mutant alone.

Molecular biology

Standard molecular biological techniques were used (Ausubel et al., 1987; Sambrook, 1989). Oligonucleotide primer sequences used for PCR are available upon request. The sequences of all coding regions of clones derived using PCR in this work were determined to ensure that no errors were introduced. The *osm-6::gfp* transgene was produced by fusing the *osm-6* promoter (bases 2680-2373 of cosmid F58H1) produced by PCR from *C. elegans* genomic DNA upstream of *gfp*. *osm-6::gfp* transgenic lines were constructed by microinjection at a concentration of 30 ng/μl.

Construction and analysis of constitutively-active *rac(G12V)* transgenes

Each *rac*-coding region, including initiator ATG, introns and stop codon, was amplified by PCR from genomic DNA: *ced-10* (bases 36,193-34,079 of cosmid C09G12); *mig-2* (bases 20,146-21,722 of cosmid C35C5); and *rac-2* (bases 105-1957 of cosmid K03D3). Each coding region was placed downstream of the *osm-6* promoter and the *unc-115* promoter. The G12V mutation (G16V in *mig-2*) was introduced into the *ced-10-*, *mig-2-* and *rac-2*-coding regions using the Quikchange Site-Directed Mutagenesis System (Stratagene, La Jolla, CA). *Rac* transgenes were injected in germline transformation experiments at 5 ng/μl, and the *osm-6::gfp* plasmid was co-injected at 30 ng/μl. Multiple transformed lines were obtained for each construct (>3). Each line displayed similar behavior, and representative lines from each transgene are shown in Table 3.

To score the effects of *unc-115* mutation on PDE axons harboring *rac* transgenes, arrays were crossed into the *unc-115(ky275)* mutant background. At least two independent arrays consisting of each transgene were scored in the *unc-115* background with similar results. One representative line from each is shown in Table 3. Furthermore, the transgenes were re-isolated by outcrossing from *unc-115* and rescored. PDE defects were restored to a degree similar to what was observed before building the *unc-115; rac-2(G12V)* double (data not shown).

Construction and analysis of *gfp*-tagged *rac-2*

The *gfp*-coding region was placed upstream of and in frame with the *rac-2*-coding region in the *unc-115 promoter::rac-2(+)* and *unc-115 promoter::rac-2(G12V)* transgenes. Frameshifts between *gfp*- and *rac-2*-coding regions were produced by fusing *gfp* upstream of and out of frame with the *rac-2*-coding regions. *unc-115::gfp::rac-2* transgenes were microinjected at concentrations of 5 ng/μl to generate extrachromosomal arrays.

Molecular modeling and actin co-sedimentation

The program MODELLER was used to model the structure of the UNC-115 VHD from the chicken villin VHD (HP67; 1qqv.pdb). Charge distribution was determined using SYBYL program.

For actin sedimentation assays, a fragment of the C-terminal region of the *unc-115* cDNA, including the VHD-coding region (from position 1350 in F09B9.2b open reading frame sequence to the stop codon), was fused in frame to the 6-histidine moeity and DHFR in the pQE-41 vector (Qiagen, Valencia, CA). Point mutations in the VHD were constructed using the Quikchange Site-Directed Mutagenesis System (Stratagene, La Jolla, CA). The resulting 6HIS::DHFR::UNC-115 proteins were purified by standard Ni^{++} chelation chromatography (Qiagen, Valencia, CA). Actin co-sedimentation assays were based on standard procedures (Miller et al., 1991): 5 µM 6HIS::DHFR::UNC-115 protein with and without 20 µM rabbit skeletal muscle G-actin was mixed in 5 mM Tris pH 7.5, 0.2 mM ATP, 0.2 mM DTT, 0.2 mM $CaCl_2$ and actin was polymerized by adding 20 mM $MgCl_2$, 5 mM ATP, 100 mM KCl and incubating at room temperature for 1 hour. Actin filaments were sedimented by centrifugation (130,000 ***g*** for 40 minutes). The pellet was analyzed by SDS-PAGE and western blotting with anti-RGS-6HIS antibody (Qiagen, Valencia, CA).

RESULTS

Three Racs and UNC-73 GEF act in PDE axon development

We have shown previously that the three *C. elegans rac* genes *ced-10*, *mig-2* and *rac-2/3* have overlapping functions in CAN axon and D-class motor axon development (Lundquist et al., 2001). To determine if *rac* redundancy is conserved in other neurons, we analyzed the effects of *racs* on the development of the axons of the PDE neurons. The PDE neuron is also a useful model for studying axon pathfinding: PDE axon morphology is relatively simple; the PDE axons can be unambiguously distinguished from the axons of other neurons; and PDE function is not required for viability. The two PDEs are a bilaterally-symmetric pair of ciliated neurons that reside at the lateral midline in the post-deirid ganglion in the posterior of the animal (Fig. 1A) (White et al., 1986). A single, unbranched axon from the cell body extends straight ventrally to the ventral nerve cord (VNC) (Fig. 1B), where the axon bifurcates and extends anteriorly and posteriorly in a fascicle with the other PDE axon in the VNC (Fig. 1F). A ciliated dendrite that is exposed to the external environment via a pore in the hypodermis and cuticle extends dorsally from the PDE cell body (Fig. 1B).

We analyzed PDE axon morphology in *rac* single and double loss-of-function mutants. *rac-2/3* activity was perturbed using RNAi (Fire et al., 1998). The *rac-2/3* locus is composed of two nearly identical *rac* genes, and *rac-2/3(RNAi)* is predicted to reduce the function of both genes (see Lundquist et al., 2001). *ced-10*, *mig-2* and *rac-2/3(RNAi)* single mutants displayed few defects in PDE development (Table 1). Each pairwise double mutant combination of *ced-10(n1993)*, *mig-2(mu28)* and *rac-2/3(RNAi)* displayed synthetic PDE axon defects (Table 1), including axon guidance defects (the axons failed to reach the VNC and often wandered along the lateral body wall) (Fig. 1C,D) and premature axon termination and defasciculation in the ventral nerve cord (Fig. 1E,F). In addition to these defects in axon pathfinding, *rac* double mutants displayed ectopic axon formation (ectopic axons formed as branches from the main axon or emanated from the cell body) (Fig. 1G). Thus, *rac* genes

Table 1. *ced-10, mig-2, rac-2/3* and *unc-73* act in PDE* axon pathfinding

Genotype	Percent ventral axon guidance errors[†]	Percent ectopic axons[‡]
+	0	3±3
ced-10(n1993)	0	2±2
mig-2(mu28)	1±2	6±3
mig-2(gm38mu133)	1±2	4±3
rac-2/3(RNAi)	0	2±5
*ced-10(n1993*M+*); mig-2(mu28)*[§]	65±9	21±8
*ced-10(n1993*M+*); mig-2(gm38mu133)*	55±9	23±7
ced-10(n1993); rac-2/3(RNAi)	12±5	22±6
mig-2(mu28); rac-2/3(RNAi)	18±5	19±5
mig-2(gm38mu133); rac-2/3(RNAi)	21±7	15±6
unc-73(e936)	35±6	21±6
unc-73(rh40)	24±4	28±4
unc-73(e936); ced-10(n1993)	86±3	51±5
unc-73(e936); mig-2(mu28)	71±4	68±4
unc-73(e936); rac-2/3(RNAi)	55±5	67±4
unc-73(rh40); ced-10(n1993)	72±5	37±5
unc-73(rh40); mig-2(mu28)	63±5	46±5
unc-73(rh40); rac-2/3(RNAi)	50±5	38±5
unc-73(rh40); lqEx48 (rac-2(G12V))	9±3	85±4

*PDE axon morphology was scored using the integrated transgene *lqIs3*[*osm-6::gfp*].

[†]The percent of PDE axons that failed to reach the ventral nerve cord (±2× standard error of the proportion).

[‡]The percent of PDE axons that exhibited ectopic axons emanating from the cell body or branching from the main axon (±2× standard error of the proportion).

[§]M+ indicates that these animals were homozygous for *n1993*, but were derived from mothers heterozygous for *n1993*, and therefore retain wild-type maternal *ced-10* activity.

control multiple aspects of PDE axon development, including axon pathfinding (guidance, outgrowth and fasciculation), as well as suppression of ectopic axon formation. Similar results were obtained using the *mig-2(gm38mu133)* allele (Table 1). Each *rac* double mutant displayed the entire spectrum of defects, suggesting that all three *rac* genes act in each process as opposed to individual *rac* gene involvement in a single aspect of PDE axon development.

*ced-10(*M+*); mig-2* double mutants also displayed defects in PDE dendrite development (data not shown). The PDE dendrite was missing or misshapen (misguided, lacking a discernible cilium or exhibited ectopic branches) in 17% of *ced-10(*M+*); mig-2* PDE neurons. *rac-2/3(RNAi)* double mutants did not display dendrite defects.

UNC-73 is a Trio-like molecule with two DH-GEF domains, one of which, GEF1, is a Rac-GEF (Steven et al., 1998). *unc-73* acts with the three Racs in CAN and D-class axon development (Lundquist et al., 2001), and here we find that *unc-73* also affects PDE axon development. The incomplete loss-of-function mutants *unc-73(rh40)* and *unc-73(e936)* displayed PDE axon defects similar to *rac* double mutants, including axon guidance defects, axon defasciculation and premature termination in the VNC, and ectopic axon formation (Table 1). *unc-73(rh40)* and *unc-73(e936)* PDE axon pathfinding defects and ectopic axon formation were enhanced significantly by *ced-10*, *mig-2* and *rac-2/3(RNAi)* (Table 1), suggesting that *unc-73* and the three *rac* genes act together in PDE axon development. However, the fact that *rac* mutations enhance *unc-73(rh40)*, a mutation that specifically attenuates

Fig. 1. *rac* double mutants display defects in PDE axon pathfinding. Fluorescence micrographs of PDE neurons visualized using the integrated *osm-6::gfp* transgene *lqIs3* are shown. Anterior is towards the left. In A-D,G, dorsal is upwards. (E-F) Ventral aspects showing PDE axons in the ventral nerve cord (VNC). (A,B) PDE neurons in wild-type animals. (A) The left PDE cell body is indicated with an arrow. The VNC is indicated with arrowheads. The amphid and phasmid ganglia of the head and tail, respectively, are shown. The V indicates the position of the vulva. The out-of-focus spot to the left of the PDE is the out-of-focus PDE cell body from the right side of the animal. (B) A single, unbranched PDE axon extended ventrally in the post-deirid commisure to the VNC, where the axon bifurcated and extended anteriorly and posteriorly in the VNC (arrowheads). A single, unbranched dendrite with an exposed, ciliated tip extended dorsally from the PDE cell body. The broken line indicates the out-of-focus PDE axons in the VNC. (C,D) The PDE axons of *ced-10*(M+*); mig-2* animals. (C) The PDE axon failed to reach the VNC (arrowheads) and wandered along the lateral body wall. (D) The PDE axon bifurcated prematurely before reaching the VNC (arrowheads) and the axons extended anteriorly and posteriorly along the lateral body wall. (E) Wild-type PDE axons formed a tight bundle in the VNC as they extended anteriorly and posteriorly. (F) The PDE axons of a *ced-10*(M+*); mig-2* animal were defasciculated and terminated prematurely in the ventral cord. (G) The PDE axon displayed an ectopic branch (arrow). Scale bar: 20 µm in A; 10 µm in B-G.
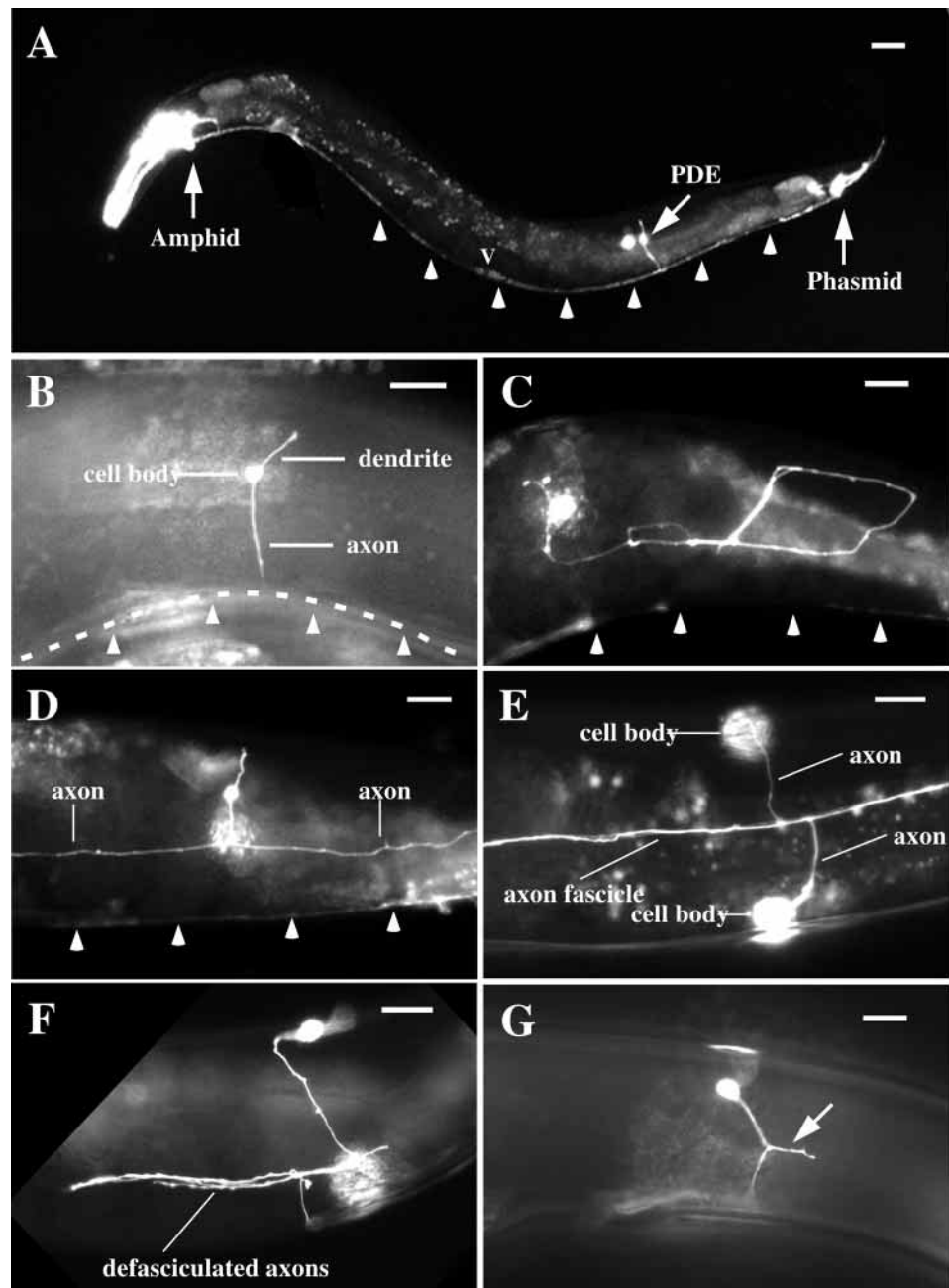
the GEF1 Rac-GEF activity of UNC-73, raises the possibility that the Racs might act in a pathway parallel to UNC-73. To determine if RAC-2 acts in the UNC-73 pathway, we tested the ability of constitutively-active *rac-2* (*rac-2* harboring the G12V mutation; see below) to suppress PDE axon defects caused by *unc-73(rh40)*. Indeed, transgenic expression of constitutively-active *rac-2* in the PDE neuron partially suppressed the PDE ventral axon guidance defects caused by *unc-73(rh40)* (Table 1). Furthermore, *unc-73(rh40)* PDE axons often wandered laterally before reaching the VNC, and this wandering was also partially suppressed by activated *rac-2* (data not shown). These data suggest that *rac-2* acts downstream of *unc-73* in the same pathway. Similar suppression of *unc-73* defects in the D-class motor axons has been observed with constitutively active *ced-10* and *mig-2* (Wu

et al., 2002). These results combined with the biochemical data that UNC-73 acts as a GEF on CED-10 and MIG-2 (Wu et al., 2002) strongly suggest that *ced-10*, *mig-2*, *rac-2/3* and *unc-73* act in the same pathway in axon pathfinding. As described by Lundquist et al. (Lundquist et al., 2001), enhancement of *unc-73(rh40)* axon pathfinding defects by *rac* mutation could be due to Rac regulation by other molecules in addition to UNC-73 or Rac regulation by a domain of UNC-73 apart from the GEF1 Rac-GEF domain.

Although these data indicate that *rac-2* acts in the *unc-73* pathway, they do not exclude the possibility that UNC-73 has additional, Rac-independent roles in PDE axon development. *unc-73(e936)* is predicted to affect multiple UNC-73 activities, including that of GEF2 Rho-GEF (Steven et al., 1998). Disruption of a *rac*-independent activity of UNC-73 by *unc-*

Table 2. *unc-115* acts with the three *rac* genes and *unc-73* in PDE* and CAN† axon pathfinding

Genotype	Percent ventral axon guidance errors	Percent ectopic axons	Percent posterior CAN axon outgrowth defects‡	Percent CAN cell migration defects§
+	0	3±3	0	5±4
unc-115(mn481)	0	5±5	0	5±4
unc-115(ky275)	0	20±5	0	10±4
unc-115(mn481); ced-10(n1993)	9±4	22±5	22±7	8±5
unc-115(ky275); ced-10(n1993)	10±4	18±5	25±6	12±4
unc-115(mn481) mig-2(mu28)	13±4	24±6	21±7	15±7
unc-115(ky275) mig-2(mu28)	15±5	20±5	21±6	10±5
unc-115(mn481); rac-2/3(RNAi)	0	4±5	0	10±5
unc-115(ky275); rac-2/3(RNAi)	0	22±8	0	9±5
unc-73(e936)	35±9	21±7	29±8	77±8
unc-73(rh40)	23±5	25±5	39±8	49±9
unc-73(e936); unc-115(ky275)	62±6	29±5	62±7	70±6
unc-73(e936); unc-115(mn481)	58±5	34±4	67±6	72±6
unc-73(rh40); unc-115(ky275)	58±7	27±5	59±8	55±8
unc-73(rh40); unc-115(mn481)	50±6	33±5	86±5	54±6
unc-73(e936); unc-115(ky275); rac-2/3(RNAi)	66±4	37±5	N.D.	N.D.
unc-73(rh40); unc-115(ky275); rac-2/3(RNAi)	53±7	31±5	N.D.	N.D.

*PDE axons were scored as described in Table 1.

†CAN axon morphology and cell body position was assessed using the integrated transgene *lqIs10*[*ceh-10::gfp*] (Lundquist et al., 2001).

‡The percentage of posterior CAN axons that failed to extend past the post-deirid ganglion is shown (±2× standard error of the proportion) (see Lundquist et al., 2001).

§The percentage of CAN cell bodies that failed to reach the region of the vulva (±2× standard error of the proportion) (see Lundquist et al., 2001).

73(e936) might contribute to *rac* enhancement of *unc-73(e936)*.

Dendrite development was also perturbed by *unc-73(rh40* and *e936*) and these defects were enhanced by *ced-10* and *mig-2* (data not shown).

UNC-115 acts with the Racs and UNC-73 in PDE and CAN axon pathfinding

unc-115 mutations cause defects in axon pathfinding and *unc-115* encodes a putative actin-binding protein (Lundquist et al., 1998). Racs are thought to mediate cellular morphogenesis in part by regulating the structure and dynamics of the actin cytoskeleton (Hall, 1998). To determine if *unc-115* acts with *rac* genes in axon pathfinding, we analyzed the CAN and PDE axons of double loss-of-function mutants of *unc-115* with *ced-10*, *mig-2* and *rac-2/3(RNAi)*. Neither *unc-115(ky275)*, a putative *unc-115* null allele, nor *unc-115(mn481)*, an incomplete loss-of-function allele, caused defects in CAN axon pathfinding (Table 2) [for a description of CAN axon pathfinding and defects see Lundquist et al. (Lundquist et al., 2001)]. However, *unc-115* animals displayed weak PDE axon guidance defects: 12% of *unc-115(ky275)* PDE axons (*n*=174) and 6% of *unc-115(mn481)* PDE axons (*n*=189) wandered laterally (>45°C from straight ventrally) on their trajectory to the VNC. All *unc-115* PDE axons eventually reached the VNC. Furthermore, *unc-115* mutants alone displayed ectopic PDE axons (20% of PDEs in *unc-115(ky275)*) (Table 2). Thus, *unc-115* mutations alone had weak effects on PDE axon development, most notably ectopic axon formation.

We found that *unc-115* synergized with *ced-10* and *mig-2* but not *rac-2/3* in CAN and PDE axon pathfinding. *unc-115; ced-10* and *unc-115 mig-2* double mutants were viable and fertile, but displayed synthetic defects, including a withered tail (Wit), similar to but weaker than *rac* double mutants and *unc-73* animals. The Wit phenotype is associated with perturbed CAN neuron development (Forrester et al., 1998) and indeed, *ced-10; unc-115* and *mig-2 unc-115* animals displayed failure of the

posterior CAN axon to extend into the tail due to axon wandering or premature termination (Table 2). Furthermore, *unc-115; ced-10* and *unc-115 mig-2* animals displayed synthetic PDE defects, including ventral axon guidance errors (Table 2) and axon defasciculation in the VNC (data not shown). These data indicate that *unc-115* has overlapping function with *ced-10* and *mig-2* in CAN and PDE axon pathfinding.

By contrast, the CAN and PDE axons of *unc-115; rac-2/3(RNAi)* animals resembled those *unc-115* alone (Table 2), suggesting that *unc-115* and *rac-2/3* affect the same pathway in CAN and PDE axon pathfinding, possibly a pathway in parallel to *mig-2* and *ced-10*. However, we cannot rule out the possibility that *unc-115* also acts in the *ced-10* pathway, because *ced-10(n1993)* is not a null allele (Soto et al., 2002) (E. A. L., unpublished results).

In addition, we found that *unc-115* acts with *unc-73* in axon pathfinding. *unc-115(ky275)* and *unc-115(mn481)* mutations significantly enhanced the CAN and PDE axon pathfinding defects caused by *unc-73(e936)* and *unc-73(rh40)* mutations (Table 2), including CAN posterior guidance errors and PDE ventral guidance errors. PDE defects of *unc-115; unc-73* double mutants were not further enhanced by *rac-2/3(RNAi)* (Table 2), confirming that *unc-115* and *rac-2/3* act in the same pathway. Taken together, these results indicate that *unc-115* acts with the *rac* genes and *unc-73* to mediate CAN and PDE axon pathfinding.

While *unc-115* and *unc-73* mutants and *rac* double mutants displayed ectopic axon formation, double mutants of *unc-115* with *ced-10*, *mig-2* and *unc-73* did not display enhanced ectopic axon formation (Table 2). Possibly, *unc-115* acts specifically with *rac-2/3* in axon pathfinding and with all three *rac* pathways in the suppression of ectopic axon formation.

The three *racs* and *unc-73* affect other actin-based morphogenetic processes, including migration of the CAN cell body (Lundquist et al., 2001). *unc-115* alone or in double mutant combinations with the *racs* and *unc-73* had no effect
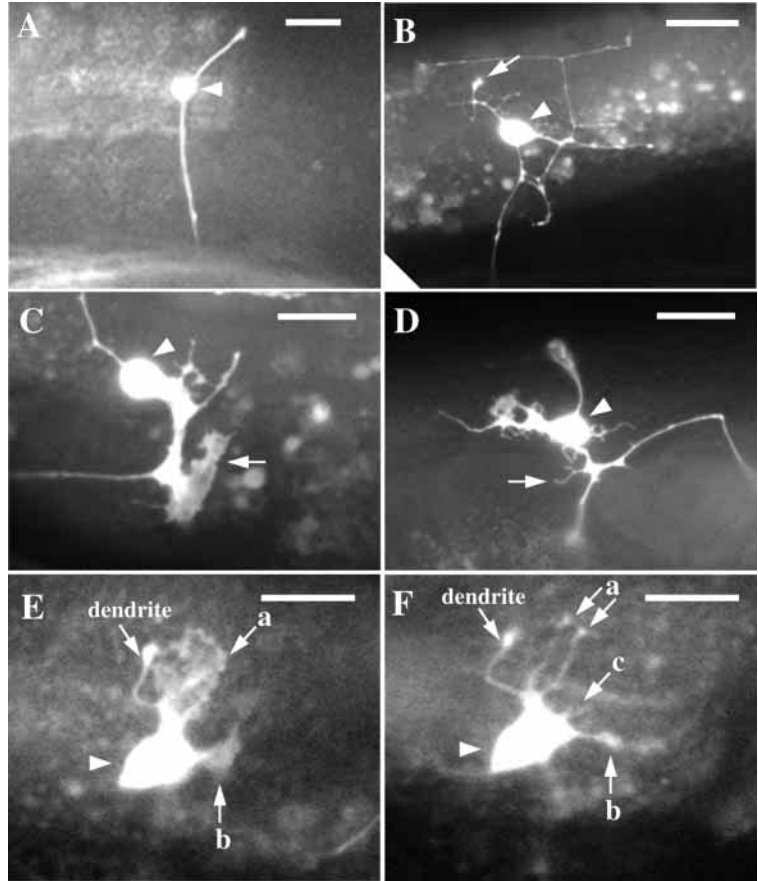
Fig. 2. Constitutively-active Racs induce ectopic morphogenetic structures in the PDE neuron. Fluorescense micrographs of PDE neurons from adult animals harboring an *osm-6::gfp* transgene. Anterior is towards the left and dorsal is upwards. The PDE cell bodies are indicated by arrowheads. (A) A wild-type PDE neuron displayed a single, unbranched axon extending to the ventral nerve cord (image is the same as in Fig. 1B). (B-F) PDE neurons of animals harboring a *rac-2(G12V)* transgene. (B) A *rac-2(G12V)* PDE neuron displayed ectopic axon branching and ectopic axons extending from the cell body. The ciliated dendrite (cilium marked by an arrow) also displayed ectopic branches. (C) A PDE neuron displayed a large, sheet-like plasma membrane extension (arrow). (D) A PDE neuron exhibited numerous thin, finger-like plasma membrane extensions (arrow). (E,F) A PDE neuron displayed two ectopic lamellipodia-like extensions (a and b) that were dynamic over time. (F) After 2 hours, one sheet-like extension (a) had ramified into two thinner neurite-like structures and another (b) had narrowed and elongated. New filopodia-like projections from the cell body not seen in E are indicated (c). Scale bars: 5 μm.

on CAN cell migration (Table 2). Indeed, *unc-115* doubles with *ced-10*, *mig-2* and *unc-73* showed no enhanced CAN cell migration defect despite enhanced CAN axon pathfinding defects. *ced-10*, *mig-2* and *rac-2/3* also control the migrations of the distal tip cells of the hermaphrodite gonad, and *ced-10* and *rac-2/3* are involved in phagocytosis of cells undergoing programmed cell death (Lundquist et al., 2001; Reddien and Horvitz, 2000). *unc-115* had no effect on distal tip cell migration or phagocytosis alone or in any double mutant combination with the *racs* and *unc-73* (P. Reddien, personal communication). Thus, *unc-115* is required for CAN and PDE axon pathfinding but is apparently not involved in CAN and distal tip cell migration and cell corpse phagocytosis.

Constitutively active Racs dominantly perturb PDE morphogenesis

In order to understand the molecular relationships UNC-115 and the three Racs, we studied the effects of constitutively active Racs on axon pathfinding. The glycine to valine mutation at position 12, which is canonical for constitutive activation of Ras superfamily GTPases, attenuates GTPase activity, thus favoring the GTP-bound, active state (Bourne et al., 1991). *mig-2(rh17)*, an allele with the equivalent *G16V* activating mutation, disrupts HSN and CAN axon pathfinding, and *ced-10(G12V)* dominantly perturbs CAN axon pathfinding and cell migration (Lundquist et al., 2001; Zipkin et al., 1997). To test if constitutively active *rac-2* can also dominantly perturb axon pathfinding, we constructed a transgene containing the *rac-2*-coding region harboring the *G12V*

mutation under the control of the *osm-6* promoter. The *osm-6* promoter is expressed exclusively in ciliated neurons, including PDE, and shows no other discernible expression (Collet et al., 1998). Similar constructs were made using the *ced-10(G12V)*- and *mig-2(G16V)*-coding regions [collectively referred to as the *rac(G12V)* transgenes], as well as the wild-type coding region of each *rac*. Animals harboring the *rac-2(G12V)* transgene displayed dominant defects in PDE axon development that resembled the defects of *rac* double loss-of-function mutants, including axon guidance errors (Table 3), axon defasciculation and ectopic axon formation (Fig. 2A,B; Table 3). *ced-10(G12V)*, *mig-2(G12V)* and *mig-2(rh17)* showed similar defects (Table 3). The pathfinding and fasciculation errors caused by the *rac(G12V)* transgenes were generally weaker than the equivalent defects caused by *rac* loss-of-function, whereas ectopic axon formation was generally more severe in *rac(G12V)* animals than in the *rac* loss-of-function mutants (compare Table 2 with Table 3, and Fig. 1E with Fig. 2A,B). The PDE dendrite also displayed ectopic branching in each of the three *rac(G12V)* animals (Fig. 2B). The wild-type versions of each *rac* transgene caused PDE axon defects similar to but weaker than the *rac(G12V)* transgenes, most often weak ectopic axon formation (Table 3). *rac(G12V)* expression driven by a different promoter, the neuron-specific *unc-115* promoter, caused similar defects (data not shown).

These data indicate that Rac(G12V) molecules dominantly perturb PDE axon development. Several lines of evidence suggest that *rac(G12V)* transgenes produced gain-of-function,

Table 3. PDE* axon pathfinding defects and ectopic plasma membrane extensions caused by constitutively active *rac(G12V)* mutant transgenes

Genotype	Percent ventral axon guidance errors[†]	Percent ectopic axons[‡]	Percent abnormal cellular morphology[§]
+	0	2±3	0
ced-10(G12V) (lqEx74)	3±3	100	23±7
ced-10(+) (lqEx91)	0	8±6	0
mig-2(G16V) (lqEx96)	2±4	25±10	5±4
mig-2(rh17)	12±5	51±11	2±4
mig-2(+) (lqEx93)	0	11±4	0
rac-2(G12V) (lqEx48)	1±1	67±6	12±4
rac-2(+) (lqEx85)	0	3±2	1±2
unc-115(ky275)	0	20±5	0
unc-115(ky275); ced-10(G12V)	12±3	100	31±5
unc-115(ky275); mig-2(G16V)	4±2	52±6	12±4
unc-115(ky275) mig-2(rh17)	15±4	43±7	4±3
unc-115(ky275); rac-2(G12V)	0	26±5	1±1

*PDE axon morphology was scored using the integrated transgene *lqIs3[osm-6::gfp]*.

[†]The percent of PDE axons that failed to reach the ventral nerve cord (±2× standard error of the proportion).

[‡]The percent of PDE axons that exhibited ectopic axons emanating from the cell body or branching from the main axon (±2× standard error of the proportion).

[§]The percentage of PDE neurons exhibiting ectopic morphological defects including plasma membrane sheet-like protrusions and thin extensions (±2× standard error of the proportion).

constitutively active Rac molecules: similar mutations in other Ras superfamily GTPases produce constitutive activation; the effects of *rac(G12V)* were dominant to wild type; the effects of *ced-10(G12V)* did not require wild-type *ced-10* (data not shown); and the effects of *rac(G12V)* transgenic expression were more severe than *rac(+)* transgenic expression.

Constitutively active Racs induce ectopic plasma membrane extensions

In addition to pathfinding defects and ectopic axon formation, constitutively active *racs* caused PDE cell shape alterations not seen in *rac* loss-of-function double mutants. Animals harboring any of the three *rac(G12V)* transgenes displayed sheet-like extensions of plasma membrane and multiple, thin processes emanating from the cell bodies, axons and dendrites (Fig. 2C,D). Ectopic axons often emanated from the sheet-like extensions. The thin processes were generally thinner and shorter than the normal or ectopic axons and were often observed at the edges of the sheet-like membrane extensions. Despite abnormal cellular morphology, the PDE axons usually completed their extensions to the VNC.

rac(G12V)-induced ectopic extensions displayed dynamic morphology even in adult animals (Fig. 2E,F). For example, the sheet-like structures were observed to form single or multiple neurite-like extensions, and the thin processes were apparently extended and retracted over time. These results demonstrate that constitutively active *racs* induced dynamic cellular structures, plasma membrane extensions and thin processes, not seen in *rac*, *unc-73* or *unc-115* loss-of-function mutants. However, these structures resemble lamellipodia and filopodia normally found on growth cones during axon outgrowth (Knobel et al., 2001). Possibly, Rac(G12V) molecules ectopically induce these morphogenetic structures.

UNC-115 is required for the morphogenetic effects of constitutively-active RAC-2

The loss-of-function studies described above place *unc-115* in the *rac-2/3* pathway. To test if UNC-115 acts downstream of RAC-2, we determined if loss of *unc-115* function could suppress the effects of constitutively active *rac-2(G12V)*. We found that the null mutation *unc-115(ky275)* suppressed the dominant effects of *rac-2(G12V)* (Table 3). The strong ectopic axon formation induced by *rac-2(G12V)* was suppressed by *unc-115(ky275)* to a level similar to *unc-115(ky275)* alone, and *unc-115(ky275)* suppressed the ectopic plasma membrane extensions induced by *rac-2(G12V)*. Whereas the axon pathfinding defects caused by *rac-2(G12V)* were weak (1%), we saw no axon pathfinding defects in *unc-115(ky275); rac-2(G12V)* double mutants. By contrast, *unc-115(ky275)* did not suppress the effects of constitutively-active *ced-10(G12V)*, *mig-2(G16V)* or *mig-2(rh17)* (Table 3). Instead, *unc-115(ky275)* slightly enhanced the effects of *ced-10(G12V)* and *mig-2(G16V)*. These results indicate that UNC-115 activity mediates the effects of constitutively active RAC-2(G12V). Although it is possible that RAC-2(G12V) perturbs a process in which Racs are not normally involved, the loss-of-function data that place *rac-2/3* and *unc-115* in the same pathway combined with *unc-115* suppression of *rac-2(G12V)* strongly suggest that UNC-115 acts downstream of RAC-2 in PDE axon development.

GFP::RAC-2 accumulates at the plasma membrane

Rho GTPases, including Racs, are anchored to the plasma membrane by covalent attachment of prenyl group mediated by a C-terminal CAAX box (Zhang and Casey, 1996), and GFP::MIG-2 and GFP::CED-10 accumulate at the plasma membrane (Lundquist et al., 2001; Zipkin et al., 1997). The potential RAC-2 polypeptide contains a consensus C-terminal CAAX box (CTVL). To determine if RAC-2 accumulates at the plasma membrane, a *rac-2* transgene was generated that consisted of the wild-type *rac-2*-coding region fused in-frame downstream of the green fluorescent protein (*gfp*) (Chalfie et al., 1994) coding region (Fig. 3A). This transgene is predicted to encode a full-length RAC-2 molecule tagged with GFP at the N terminus. The expression of the *gfp::rac-2* transgene was placed under the control of the *unc-115* promoter, which is expressed in most if not all neurons and neuroblasts (Lundquist et al., 1998). Animals harboring the *unc-115::gfp::rac-2* transgene showed expression of GFP::RAC-2 that accumulated at the cell margins of neuroblasts and neurons as well as in the nerve ring (Fig. 3B-D). The nerve ring is composed of the axons of many neurons (White et al., 1986), and nerve ring accumulation suggests that GFP::RAC-2 localized to the plasma membranes of axons. GFP::CED-10 and GFP::MIG-2 show similar plasma membrane and nerve ring accumulation (Lundquist et al., 2001; Zipkin et al., 1997). Wild-type *rac-2* (Fig. 3) and *rac-2(G12V)*-coding regions displayed indistinguishable localization, and *gfp::rac-2(G12V)* caused dominant effects on PDE development as described above (data not shown). Expression of GFP from a transgene that contained a frameshift between the *gfp*- and *rac-2*-coding regions failed to accumulate at the cell margins and in the nerve ring (Fig. 3E-G) and instead was uniformly distributed in the cytoplasm, indicating that RAC-2 sequences mediate accumulation of GFP::RAC-2 at the plasma membrane, presumably via C-terminal CAAX motif.

Fig. 3. GFP::RAC-2 is anchored to the plasma membrane. (A) A diagram of the *unc-115::gfp::rac-2* transgene and the putative GFP::RAC-2 molecule produced from this transgene are shown. The neuron-specific *unc-115* promoter was used to drive expression of *gfp* fused in-frame to the entire wild-type *rac-2*-coding region, including introns. This transgene is predicted to produce a RAC-2 molecule with an N-terminal GFP tag. The CAAX motif at the C terminus of RAC-2 might direct covalent addition of a prenyl group and subsequent anchorage of the molecule to the plasma membrane. The position of the frame shift mutation in *unc-115::gfp::(FS)::rac-2* is indicated. (B,D) Wild-type animals harboring the *unc-115::gfp::rac-2* transgene. GFP::RAC-2 accumulated at the cell margins of neuroblasts of the 1.5-fold embryo in (B) and of neurons in the L1 larva in C. The animal in C displayed strong GFP::RAC-2 accumulation in the nerve ring. (D) A magnified image of the area around the nerve ring of the animal in (C). Neuron cell bodies with GFP::RAC-2 at their periphery are evident. (E,G) Wild-type animals of the same age as those in B,C harboring the *unc-115::gfp::(FS)rac-2* transgene that contains a frameshift mutation between *gfp* and *rac-2* sequences. This transgene is predicted to encode a full-length GFP without RAC-2 sequences. GFP accumulation was no longer observed at cell margins of neuroblasts and neurons and was observed throughout the cytoplasm, and nerve ring accumulation was abolished. (G) A magnified view of the area around the nerve ring of the animal in F. Scale bars: in B 10 µm for B,C,E,F; in D 2 µm for D,G.
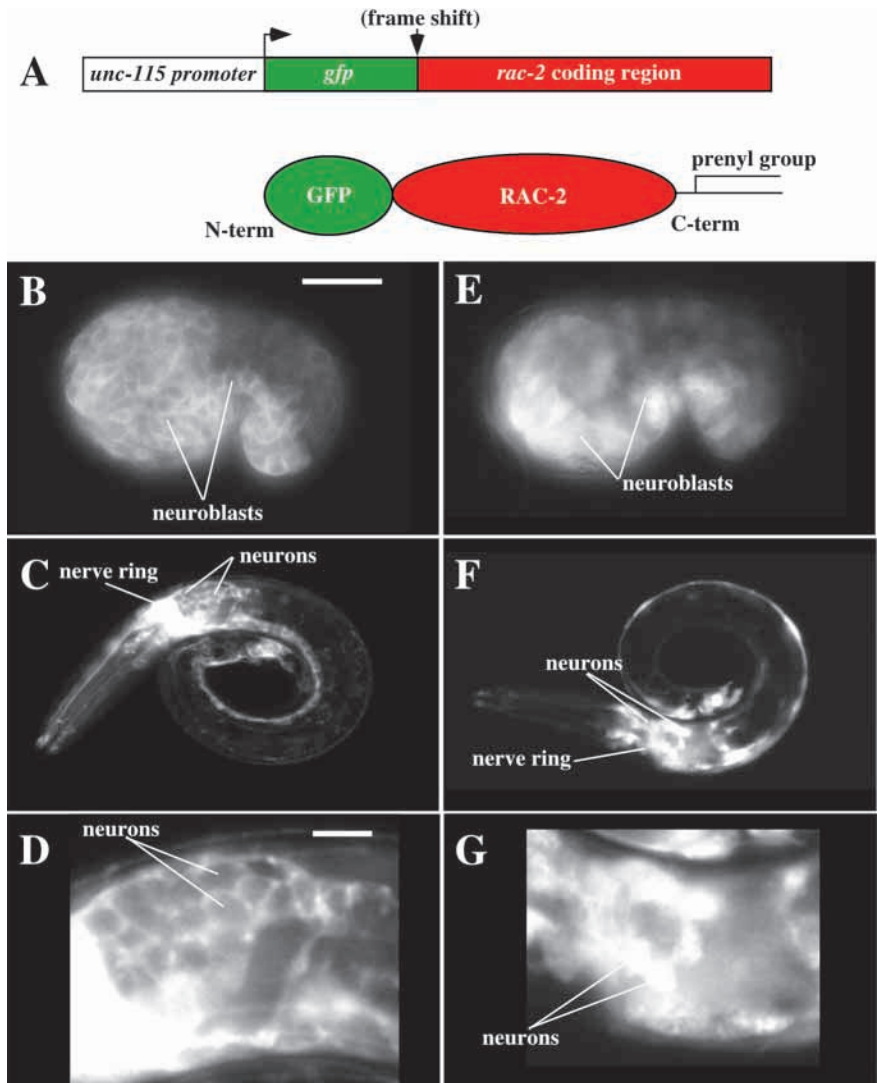
UNC-115 is an actin-binding protein

The predicted UNC-115 polypeptide consists of three N-terminal LIM domains and a C-terminal region similar to the actin-binding headpiece domain of villin (VHD) (Fig. 4A,B) (Lundquist et al., 1998). Not all VHDs can bind to actin, and those VHDs with demonstrated actin-binding ability have conserved basic residues that form a 'positive patch' that might mediate molecular contacts with actin (Vardar et al., 2002). We modeled the structure of the UNC-115 VHD based upon the NMR structure of the chicken villin VHD (called HP67) (Fig. 4B,C). The UNC-115 VHD had hallmark features of all VHDs, including a hydrophobic 'cap' and a charged 'crown' (Fig. 4C) (see Vardar et al., 2002). Furthermore, the UNC-115 VHD had a prominent 'positive patch' similar to other actin-binding VHDs. We next tested the ability of the UNC-115 VHD to co-sediment with F-actin in vitro. A bacterially expressed fragment of UNC-115 containing the VHD sedimented in the presence of but not in the absence of actin filaments (Fig. 4D). We generated a mutant form of the UNC-115 VHD in which basic residues that contribute to the 'positive patch' were changed to acidic residues (Fig. 4B,C). This mutant VHD failed to co-sediment with actin filaments (Fig. 4D). These results demonstrate that the UNC-115 VHD is an actin filament binding domain.

DISCUSSION

While some downstream effectors of Rac signaling in morphogenesis are known, many remain to be identified. Furthermore, questions remain about how multiple Racs and effector molecules are deployed during development to mediate specific morphogenetic events such as axon pathfinding. We have identified and characterized UNC-115 as a new downstream cytoskeletal effector of Rac signaling in axon pathfinding.

Three *C. elegans rac* genes define three overlapping pathways that regulate the development of CAN and D-class axons, and *unc-73 Trio GEF* is likely to control all three *rac* pathways in this process (Wu et al., 2002; Lundquist et al., 2001). Furthermore, UNC-73 Trio is known to act as a GEF for multiple Racs, including the canonical Racs and the MIG-2-like Racs (Wu et al., 2002; Newsome et al., 2000; Steven et al., 1998). We have shown that the three *racs* act redundantly

Fig. 4. The villin headpiece domain of UNC-115 binds to actin filaments. (A) The 639-residue UNC-115 polypeptide. The N terminus consists of three LIM domains and the C-terminus is similar to the headpiece domain of villin (VHD). The region of UNC-115 used in actin-binding assays is indicated by a bar below the diagram. (B) An alignment of the UNC-115 VHD and chicken villin VHD (Gg HP67). Basic residues in the UNC-115 VHD are in blue, and those that were changed to glutamic acid residues to produce the VHD mutant protein are shown with asterisks. The leucine and tryptophan residues that form a hydrophobic 'cap' (see below) are boxed. (C) A structural model of the UNC-115 VHD based upon the NMR structure of Gg HP67

(Varder et al., 2002) (see Materials and Methods). Blue, basic groups; red, acidic groups; white, neutral groups. Shown are the 'cap' formed by the leucine and tryptophan boxed in B, the charged 'crown' (broken line), and the 'positive patch' formed by basic residues (Vardar et al., 2002). The locations of basic residues that were changed to glutamic acid residues in UNC-115 VHD mutant protein are indicated by asterisks. (D) A western blot showing that the UNC-115 VHD bound to actin. Equimolar amounts (5 μM) of wild-type and VHD mutant 6HIS::DHFR::UNC-115 (~46kD) were mixed with actin filaments, which were then sedimented (see Materials and Methods). Wild-type 6HIS::DHFR::UNC-115 co-sedimented in the presence but not in the absence of actin filaments. Mutant 6HIS::DHFR::UNC-115 (see B) failed to co-sediment with actin filaments.
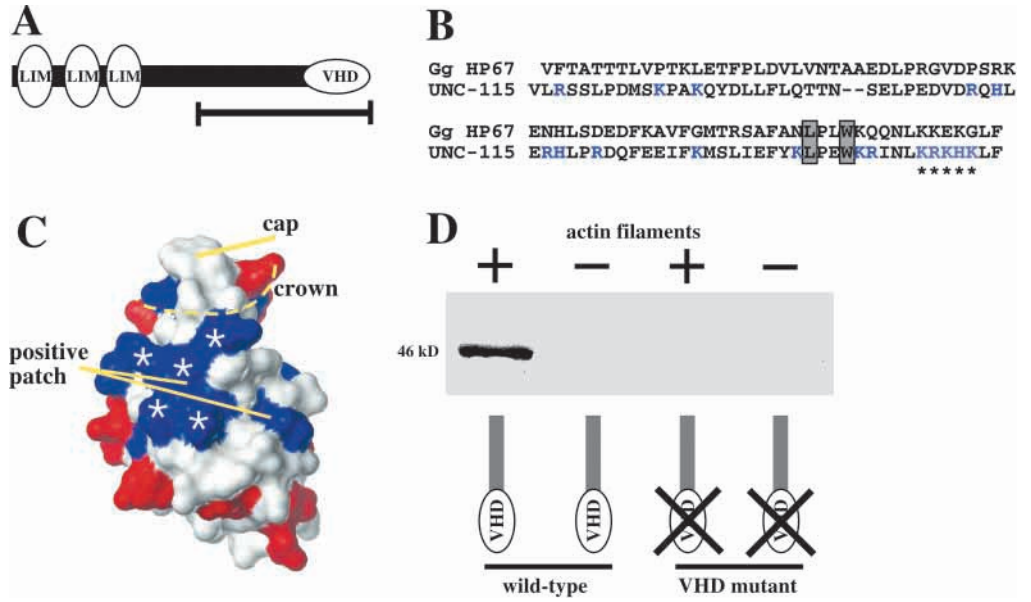
in PDE axon development. Multiple aspects of PDE development are affected by *rac* loss-of-function, including axon guidance, axon fasciculation and axon outgrowth as well as suppression of ectopic axon formation, indicating that *rac* genes control multiple aspects of axon development. We also provide evidence that the three *racs* act with *unc-73* in axon pathfinding: each *rac* loss-of-function mutation enhanced weak *unc-73* mutations and *rac-2(G12V)* suppressed *unc-73(rh40)*. Together with results showing that UNC-73 GEF1 acts as a GEF on CED-10 and MIG-2 (Wu et al., 2002), these data indicate that the *racs* and *unc-73* act in the same pathway in PDE axon pathfinding.

unc-115 acts with the *rac* genes and *unc-73 Trio* in CAN and PDE axon pathfinding

UNC-115 is a molecule similar to the human actin-binding protein abLIM/limatin (Lundquist et al., 1998; Roof et al., 1997) and consists of three N-terminal LIM domains, which are thought to mediate protein-protein interactions (Dawid et al., 1998), and a C-terminal villin headpiece domain, an actin-binding domain found in a variety of proteins (Vardar et al., 2002). UNC-115 is required for pathfinding of many but not all axons in *C. elegans* (Lundquist et al., 1998), and dominant-negative abLIM/limatin can perturb RGC axon pathfinding in the developing mouse visual system (Erkman et al., 2000). UNC-115 might act as a cytoskeletal adapter protein that interacts with actin via the VHD and with other molecules via the LIM domains. We show that UNC-115 acts downstream of Rac signaling during axon pathfinding, suggesting that UNC-115 might adapt Rac activity to the growth cone actin cytoskeleton.

In *C. elegans*, *unc-115* is expressed in most if not all neurons throughout development, yet many neurons display normal or near-normal axon pathfinding and development in *unc-115* null mutants (Lundquist et al., 1998). Our results explain this paradoxical observation by demonstrating that *unc-115* acts in the *rac-2/3* branch of the tripartite *rac* cascade and has overlapping function with the *ced-10* and *mig-2* pathways in axon pathfinding. However, *ced-10(n1993)* is not a null allele
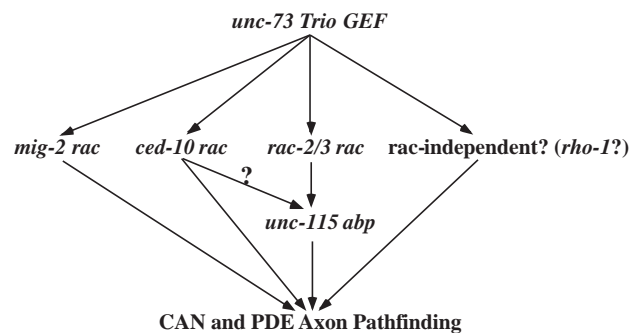
Fig. 5. UNC-115 acts downstream of Rac signaling in CAN and PDE axon pathfinding. The genetic relationships between the three *racs*, *unc-73* and *unc-115* are shown. Arrows indicate that the genes act in the same pathway. Three *rac* genes *ced-10*, *mig-2* and *rac-2/3*, define three parallel pathways with overlapping function. *unc-73* acts in all three pathways, and *unc-115* acts downstream of *rac-2* and possibly *ced-10*. *unc-73* might have *rac*-independent roles in axon pathfinding possibly mediated by the *rho-1* gene that encodes the single *C. elegans* Rho GTPase. GEF, GTP exchange factor; abp, actin-binding protein.

and *unc-115* might enhance *ced-10(n1993)*. Therefore, *unc-115* might act in both the *rac-2/3* and *ced-10* pathways. If this is the case, then there must be other genes that act in parallel to *unc-115* in the *ced-10* pathway, as the *unc-115* null phenotype is viable and fertile and does not resemble the *ced-10* null. Although *unc-115* might act in the *rac-2/3* pathway in axon pathfinding, *unc-115* might act with all three *racs* in the suppression of ectopic axons, as *unc-115* mutants alone display ectopic axon formation that is not enhanced by mutations in the three *rac* genes.

The genetic relationships between the *rac* genes, *unc-73* and *unc-115* in axon pathfinding are shown in Fig. 5. Although our results indicate that UNC-73 controls the three Racs in axon development, they do not exclude the possibility that UNC-73 has additional, Rac-independent effects on axon pathfinding. In addition to the GEF1 Rac GEF domain, UNC-73 has a second GEF domain (GEF2) that acts on the Rac-related small GTPase Rho (Spencer et al., 2001; Steven et al., 1998). Possibly, *rho-1*, the single *C. elegans* gene that encodes Rho, acts downstream of *unc-73* in parallel to the *racs* to control PDE axon development.

We found that *unc-115* was not required for other morphogenetic events involving the *racs* and *unc-73*, including migration of the CAN cell bodies, migration of the distal tip cell of the hermaphrodite gonad and phagocytosis of cell corpses undergoing programmed cell death. *unc-115* might be a *rac* effector that acts specifically in axon pathfinding. Possibly, other genes with roles similar to *unc-115* act with the *racs* and *unc-73* in other morphogenetic events.

Constitutive Rac signaling can induce plasma membrane extensions in neurons

PDE neurons of animals harboring *ced-10(G12V)*, *mig-2(G16V)* and *rac-2(G12V)* constitutively-active transgenes displayed ectopic structures not seen in *rac* loss-of-function mutants, including extensive networks of ectopic axons. *rac(G12V)* animals also displayed ectopic plasma membrane extensions consisting of large, sheet-like structures, as well as thin, finger-like projections emanating from cell bodies, axons and dendrites. These structures were dynamic over time, even in adult animals. Although we have no direct evidence of the nature of these structures, their form and dynamics resemble actin cytoskeleton-based lamellipodia and filopodia found in growth cones of developing animals (Knobel et al., 1999). Rac activity is known to induce ectopic lamellipodia in cultured cells (Ridley et al., 1992), consistent with our observation of lamellipodia-like structures induced by Rac activity in vivo. However, we also observed filopodia-like extensions induced by Rac activity in PDE neurons, suggesting that Rac activity might induce the formation of both lamellipodia-like and filopodia-like structures in vivo. Possibly, Rac activity is required to produce these structures in growth cones and is normally precisely controlled by upstream regulators such as UNC-73 Trio.

Loss of *rac* function caused both axon pathfinding defects and ectopic axon formation. Constitutive *rac* activity also caused both axon pathfinding defects and ectopic axon formation, suggesting that Rac activity is required for both axon initiation and growth, as well as for inhibition of superfluous axons and branches. Alternatively, constitutive activation of one *rac* might trigger a negative regulatory system that attenuates all *rac* signaling. If *racs* are required for both axon initiation and axon suppression, the mechanism of ectopic axon formation caused by *rac* loss-of-function and *rac(G12V)* constitutive activation might be distinct: *rac* loss-of-function ectopic axons might be due to a failure to prune spurious axon initiation, whereas Rac(G12V) activity might induce ectopic axons via uncontrolled axon initiation.

UNC-115 activity is required for the effects of constitutively-active RAC-2(G12V)

Rac(G12V) molecules might persistently signal to their downstream effectors leading to the ectopic formation of cellular structures that are normally precisely controlled during axon pathfinding. We found that UNC-115 is required for all of the morphogenetic effects of RAC-2(G12V), indicating that UNC-115 acts downstream of RAC-2 to mediate these events and that UNC-115 is normally involved in the formation of Rac-induced membrane extensions.

unc-115 did not suppress *mig-2(G12V)* or *ced-10(G12V)*, consistent with the idea that UNC-115 acts with RAC-2 specifically. However, *unc-115* might act in the *ced-10* pathway in parallel to another gene with overlapping function. Possibly, *unc-115* does not suppress *ced-10(G12V)* because *ced-10(G12V)* can exert its influence through a downstream effector gene that is redundant with *unc-115*. Inherent in both models is the existence of other molecules, possibly other actin-binding proteins, that act downstream of MIG-2 and CED-10 in parallel to UNC-115. *unc-115* is the only member of the *unc-115/abLIM* family present in the *C. elegans* genome (The *C. elegans* Genome Sequencing Consortium, 1998), so *unc-115* redundancy will be at the functional level and not a result of homologous genes (as observed with *rac* redundancy).

UNC-115 is a new downstream cytoskeletal effector of Rac signaling

Our results show that UNC-115 is required for the formation of plasma membrane extensions that resemble lamellipodia and filopodia, actin-based structures that normally regulate cell shape. We show that the modeled UNC-115 VHD structure contains a 'positive patch' found in other actin-binding VHDs (Varder et al., 2002) and that the UNC-115 VHD binds to actin filaments in vitro, indicating that UNC-115 is an actin-binding protein. UNC-115 might control axon pathfinding by directly interacting with the actin cytoskeleton of growth cones.

The loss-of-function and epistasis suppression experiments described here implicate UNC-115 as a downstream effector of Rac signaling in axon pathfinding. In response to a signal (possibly an extracellular guidance signal), UNC-73 Trio might act on all three Racs, which then influence the actin cytoskeleton to achieve morphogenetic change underlying growth cone outgrowth and steering. UNC-115 might respond to RAC-2 and possibly CED-10 by binding to and modulating the actin cytoskeleton of the growth cone. Other actin binding proteins might act redundantly with UNC-115 to mediate cytoskeletal change in response to CED-10 and MIG-2 signals. Furthermore, UNC-115 appears to act downstream of Rac signaling specifically in axon pathfinding, indicating that Racs might use different downstream effectors to mediate different morphogenetic events.

REFERENCES

Anderson, P. (1995). Mutagenesis. In Caenorhabditis elegans*: Modern Biological Analysis of an Organism* (*Methods in Cell Biology*), Vol. 48 (ed. H. F. Epstein and D. C. Shakes), pp. 31-58. San Diego, CA: Academic Press.

Ausubel, F., Brent, R., Kingston, R., Moore, D., Seidman, J., Smith, J. and Struhl, K. (ed.) (1987). *Current Protocols in Molecular Biology*. John Wiley and Sons.

Awasaki, T., Saito, M., Sone, M., Suzuki, E., Sakai, R., Ito, K. and Hama, C. (2000). The *Drosophila trio* plays an essential role in patterning of axons by regulating their directional extension. *Neuron* **26**, 119-131.

Azuma, T., Witke, W., Stossel, T. P., Hartwig, J. H. and Kwiatkowski, D. J. (1998). Gelsolin is a downstream effector of rac for fibroblast motility. *EMBO J.* **17**, 1362-1370.

Bateman, J., Shu, H. and van Vactor, D. (2000). The guanine nucleotide exchange factor trio mediates axonal development in the *Drosophila* embryo. *Neuron* **26**, 93-106.

Bellanger, J. M., Lazaro, J. B., Diriong, S., Fernandez, A., Lamb, N. and Debant, A. (1998). The two guanine nucleotide exchange factor domains of Trio link the Rac1 and the RhoA pathways in vivo. *Oncogene* **16**, 147-152.

Bishop, A. L. and Hall, A. (2000). Rho GTPases and their effector proteins. *Biochem J.* **348**, 241-255.

Bourne, H. R., Sanders, D. A. and McCormick, F. (1991). The GTPase superfamily: conserved structure and molecular mechanism. *Nature* **349**, 117-127.

Brenner, S. (1974). *The Genetics of* Caenorhabditis elegans. *Genetics* **77**, 71-94.

Chalfie, M., Tu, Y., Euskirchen, G., Ward, W. W. and Prasher, D. C. (1994). Green fluorescent protein as a marker for gene expression. *Science* **263**, 802-805.

Clark, S. G., Lu, X. and Horvitz, H. R. (1994). The *Caenorhabditis elegans* locus *lin-15*, a negative regulator of a tyrosine kinase signaling pathway, encodes two different proteins. *Genetics* **137**, 987-997.

Collet, J., Spike, C. A., Lundquist, E. A., Shaw, J. E. and Herman, R. K. (1998). Analysis of *osm-6*, a gene that affects sensory cilium structure and sensory neuron function in *Caenorhabditis elegans*. *Genetics* **148**, 187-200.

Dawid, I. B., Breen, J. J. and Toyama, R. (1998). LIM domains: multiple roles as adapters and functional modifiers in protein interactions. *Trends Genet.* **14**, 156-162.

Dickson, B. J. (2001). Rho GTPases in growth cone guidance. *Curr. Opin. Neurobiol.* **11**, 103-110.

Didsbury, J., Weber, R. F., Bokoch, G. M., Evans, T. and Snyderman, R. (1989). rac, a novel ras-related family of proteins that are botulinum toxin substrates. *J. Biol. Chem.* **264**, 16378-16382.

Eden, S., Rohatgi, R., Podtelejnikov, A. V., Mann, M. and Kirschner, M. W. (2002). Mechanism of Regulation of WAVE1-induced actin nucleation by Rac1 and Nck. *Nature* **418**, 790-793

Erkman, L., Yates, P. A., McLaughlin, T., McEvilly, R. J., Whisenhunt, T., O'Connell, S. M., Krones, A. I., Kirby, M. A., Rapaport, D. H., Bermingham, J. R. et al. (2000). A POU domain transcription factor-dependent program regulates axon pathfinding in the vertebrate visual system. *Neuron* **28**, 779-792.

Fire, A., Xu, S., Montgomery, M. K., Kostas, S. A., Driver, S. E. and Mello, C. C. (1998). Potent and specific genetic interference by double-stranded RNA in *Caenorhabditis elegans*. *Nature* **391**, 806-811.

Forrester, W. C., Perens, E., Zallen, J. A. and Garriga, G. (1998).

Identification of *Caenorhabditis elegans* genes required for neuronal differentiation and migration. *Genetics* **148**, 151-165.

Haataja, L., Groffen, J. and Heisterkamp, N. (1997). Characterization of RAC3, a novel member of the Rho family. *J. Biol. Chem.* **272**, 20384-20388.

Hakeda-Suzuki, S., Ng, J., Tzu, J., Dietzl, G., Sun, Y., Harms, M., Nardine, T., Luo, L. and Dickson, B. J. (2002). Rac function and regulation during *Drosophila* development. *Nature* **416**, 438-442.

Hall, A. (1998). Rho GTPases and the actin cytoskeleton. *Science* **279**, 509-514.

Kaibuchi, K., Kuroda, S. and Amano, M. (1999). Regulation of the cytoskeleton and cell adhesion by the Rho family GTPases in mammalian cells. *Annu. Rev. Biochem.* **68**, 459-486.

Kishore, R. S. and Sundaram, M. V. (2002). *ced-10 Rac* and *mig-2* function redundantly and act with *unc-73 trio* to control the orientation of vulval cell divisions and migrations in *Caenorhabditis elegans*. *Dev. Biol.* **241**, 339-348.

Kissil, J. L., Johnson, K. C., Eckman, M. S. and Jacks, T. (2002). Merlin phosphorylation by p21-activated kinase 2 and effects of phosphorylation on merlin localization. *J. Biol. Chem.* **277**, 10394-10399.

Knobel, K. M., Jorgensen, E. M. and Bastiani, M. J. (1999). Growth cones stall and collapse during axon outgrowth in *Caenorhabditis elegans*. *Development* **128**, 4079-4092.

Letourneau, P. C. (1996). The cytoskeleton in nerve growth cone motility and axonal pathfinding. *Perspect. Dev. Neurobiol.* **4**, 111-123.

Liebl, E. C., Forsthoefel, D. J., Franco, L. S., Sample, S. H., Hess, J. E., Cowger, J. A., Chandler, M. P., Shupert, A. M. and Seeger, M. A. (2000). Dosage-sensitive, reciprocal genetic interactions between the Abl tyrosine kinase and the putative GEF trio reveal trio's role in axon pathfinding. *Neuron* **26**, 107-118.

Lundquist, E. A., Herman, R. K., Shaw, J. E. and Bargmann, C. I. (1998). UNC-115, a conserved protein with predicted LIM and actin-binding domains, mediates axon guidance in *C. elegans*. *Neuron* **21**, 385-392.

Lundquist, E. A., Reddien, P. W., Hartwieg, E., Horvitz, H. R. and Bargmann, C. I. (2001). Three *C. elegans* Rac proteins and several alternative Rac regulators control axon guidance, cell migration and apoptotic cell phagocytosis. *Development* **128**, 4475-4488.

Luo, L. (2000). Rho GTPases in neuronal morphogenesis. *Nat. Rev. Neurosci.* **1**, 173-180.

Luo, L., Hensch, T. K., Ackerman, L., Barbel, S., Jan, L. Y. and Jan, Y. N. (1996). Differential effects of the Rac GTPase on Purkinje cell axons and dendritic trunks and spines. *Nature* **379**, 837-840.

Luo, L., Liao, Y. J., Jan, L. Y. and Jan, Y. N. (1994). Distinct morphogenetic functions of similar small GTPases: *Drosophila* Drac1 is involved in axonal outgrowth and myoblast fusion. *Genes Dev.* **8**, 1787-1802.

Mello, C. and Fire, A. (1995). DNA transformation. In Caenorhabdítis elegans*: Modern Biological Analysis of an Organism* (*Methods in Cell Biology*), Vol. 48 (ed. H. F. Epstein and D. C. Shakes), pp. 451-482. San Diego, CA: Academic Press.

Miller, K. G., Fields, C. M., Alberts, B. M. and Kellog, D. R. (1991). Use of actin filament and microtubule affinity chromatography to identify proteins that bind to the cytoskeleton. In *Methods in Enzymology* (ed. R. B. Vallee), pp. 303-319. San Diego, CA: Academic Press.

Newsome, T. P., Schmidt, S., Dietzl, G., Keleman, K., Asling, B., Debant, A. and Dickson, B. J. (2000). Trio combines with dock to regulate Pak activity during photoreceptor axon pathfinding in *Drosophila*. *Cell* **101**, 283-294.

Ng, J., Nardine, T., Harms, M., Tzu, J., Goldstein, A., Sun, Y., Dietzl, G., Dickson, B. J. and Luo, L. (2002). Rac GTPases control axon growth, guidance and branching. *Nature* **416**, 442-447.

Reddien, P. W. and Horvitz, H. R. (2000). CED-2/CrkII and CED-10/Rac control phagocytosis and cell migration in *Caenorhabditis elegans*. *Nat. Cell Biol.* **2**, 131-136.

Ridley, A. J., Paterson, H. F., Johnston, C. L., Diekmann, D. and Hall, A. (1992). The small GTP-binding protein rac regulates growth factor-induced membrane ruffling. *Cell* **70**, 401-410.

Roberts, A. W., Kim, C., Zhen, L., Lowe, J. B., Kapur, R., Petryniak, B., Spaetti, A., Pollock, J. D., Borneo, J. B., Bradford, G. B. et al. (1999). Deficiency of the hematopoietic cell-specific Rho family GTPase Rac2 is characterized by abnormalities in neutrophil function and host defense. *Immunity* **10**, 183-196.

Roof, D. J., Hayes, A., Adamian, M., Chishti, A. H. and Li, T. (1997). Molecular characterization of abLIM, a novel actin-binding and double zinc finger protein. *J. Cell Biol.* **138**, 575-588.

Sambrook, J., Fritsch, E. F. and Maniatis, T. (1989). *Molecular Cloning: A*

Laboratory Manual. Cold Spring Harbor, NY: Cold Spring Harbor Laboratory Press.

Soto, M. C., Qadota, H., Kasuya, K., Inoue, M., Tsuboi, D., Mello, C. C. and Kaibuchi, K. (2002). The GEX-2 and GEX-3 proteins are required for tissue morphogenesis and cell migrations in *C. elegans. Genes Dev.* **16**, 620-632.

Spencer, A. G., Orita, S., Malone, C. J. and Han, M. (2001). A RHO GTPase-mediated pathway is required during P cell migration in *Caenorhabditis elegans. Proc. Natl. Acad. Sci. USA* **98**, 13132-13137.

Steven, R., Kubiseski, T. J., Zheng, H., Kulkarni, S., Mancillas, J., Ruiz Morales, A., Hogue, C. W., Pawson, T. and Culotti, J. (1998). UNC-73 activates the Rac GTPase and is required for cell and growth cone migrations in *C. elegans. Cell* **92**, 785-795.

Sugihara, K., Nakatsuji, N., Nakamura, K., Nakao, K., Hashimoto, R., Otani, H., Sakagami, H., Kondo, H., Nozawa, S., Aiba, A. and Katsuki, M. (1998). Rac1 is required for the formation of three germ layers during gastrulation. *Oncogene* **17**, 3427-3433.

Sulston, J. and Hodgkin, J. (1988). Methods. In *The Nematode* Caenorhabditis elegans (ed. W. B. Wood), pp. 587-606. Cold Spring Harbor, New York: Cold Spring Harbor Laboratory Press.

Takenawa, T. and Miki, H. (2001). WASP and WAVE family proteins: key molecules for rapid rearrangement of cortical actin filaments and cell movement. *J. Cell Sci.* **114**, 1801-1809.

Tessier-Lavigne, M. and Goodman, C. S. (1996). The molecular biology of axon guidance. *Science* **274**, 1123-1133.

The *C. elegans* Genome Sequencing Consortium (1998). Genome sequence of the nematode *C. elegans*: a platform for investigating biology. *Science* **282**, 2012-2018.

Vardar, D., Chishti, A. H., Frank, B. S., Luna, E. J., Noegel, A. A., Oh, S. W., Schleicher, M. and McKnight, C. J. (2002). Villin-type headpiece domains show a wide range of F-actin-binding affinities. *Cell Motil. Cytoskel.* **52**, 9-21.

Weaver, A. M., Karginov, A. V., Kinley, A. W., Weed, S. A., Li, Y., Parsons, J. T. and Cooper, J. A. (2001) Cortactin promotes and stabilizes Arp2/3-induced actin filament network formation. *Curr. Biol.* **11**, 370-374.

Weed, S. A., Du, Y. and Parsons, J. T. (1998). Translocation of cortactin to the cell periphery is mediated by the small GTPase Rac1. *J. Cell Sci.* **111**, 2433-2443.

White, J. G., Southgate, E., Thomson, J. N. and Brenner, S. (1986). The structure of the nervous system of the nematode *Caenorhabditis elegans. Philos. Trans. R. Soc. Lond.* **314**, 1-340.

Wu, Y., Cheng, T., Lee, M. and Weng, N. (2002). Distinct Rac activation pathways control Caenorhabditis elegans cell migration and axon outgrowth. *Dev. Biol.* **250**, 145-155.

Xiao, G. H., Beeser, A., Chernoff, J. and Testa, J. R. (2002). p21-activated kinase links Rac/Cdc42 signaling to merlin. *J. Biol. Chem.* **277**, 883-886.

Zhang, F. L. and Casey, P. J. (1996). Protein prenylation: molecular mechanisms and functional consequences. *Annu. Rev. Biochem.* **65**, 241-269.

Zigmond, S. H. (1996). Signal transduction and actin filament organization. *Curr. Opin. Cell Biol.* **8**, 66-73.

Zipkin, I. D., Kindt, R. M. and Kenyon, C. J. (1997). Role of a new Rho family member in cell migration and axon guidance in *C. elegans. Cell* **90**, 883-894.